RSC Advances

PAPER

View Article Online
View Journal | View Issue

Cite this: *RSC Adv.*, 2024, **14**, 30045

Influences of solvents and monomer concentrations on the electrochemical performance and structural properties of electrodeposited PEDOT films: a comparative study in water and acetonitrile†

Yang Zhang, Linze Li * and Bingwei He*

Poly(3,4-ethylenedioxythiophene) (PEDOT) has emerged as a promising coating for neural electrodes especially through convenient electrodeposition methods. To investigate the influences of solvents and EDOT monomer concentrations on the electrochemical performance and structural characteristics of PEDOT, both aqueous and acetonitrile solutions were employed with varying monomer concentrations during deposition. The prepared PEDOT films were examined for the surface morphology, electrochemical performance, and chemical structures. The results showed that an increase in EDOT concentration in either solvent led to PEDOT films with improved charge storage capacity and reduced impedance magnitude. At equivalent monomer concentrations, PEDOT films generated in acetonitrile exhibited a rougher surface texture and better electrochemical performance. Notably, the growth rate of charge storage capacity of PEDOT prepared in acetonitrile relative to the deposited charge density was 2.5 times that of PEDOT prepared in water. These findings could help to the optimization of PEDOT coating preparation to enhance electrode performance.

Received 14th May 2024
Accepted 13th September 2024

DOI: 10.1039/d4ra03543g

rsc.li/rsc-advances

1. Introduction

The neural electrode serves as an essential component in neuromodulation devices and brain–computer interfaces.[1] To ensure stimulation safety and recording quality in these applications, the electrode interface must allow sufficient charge injection while maintaining low impedance.[1] In recent years, conductive polymers stood out as one of the most promising materials for the neural interface, due to their superior electrochemical properties, biocompatibility,[2–4] and versatility in applications such as DC stimulation,[5–7] drug delivery,[8,9] neurochemical detection.[10–12]

Among various conductive polymers, poly(3,4-ethylenedioxythiophene) (PEDOT) is a prominent example due to its favorable stability and biosafety.[13–15] The synthesis of PEDOT commonly involves various techniques such as chemical oxidation utilizing oxidants like Fe^{3+},[16,17] and electrochemical deposition with appropriate positive potentials.[13,18,19] The electrochemical deposition is widely used due to its convenience processing, *in situ* deposition, and controllable process to fabricate PEDOT coatings.[20,21]

The surface morphology and electrochemical performance of PEDOT films are affected by various factors during the electrochemical deposition. Recent studies have explored the influences of factors such as the types of dopant anions,[6,22,23] deposition parameters,[24] and substrate structures.[25,26] Nevertheless, the monomer concentration of EDOT and the choice of solvents also significantly affect the coating properties.[13,19] Kulandaivalu *et al.*[18] used aqueous solution as the electrolyte and observed that increasing the EDOT monomer concentration was conducive to promoting film formation and enhancing the electrochemical performance of the electrode. However, the range of EDOT concentrations explored was within 10 mM, constrained by the solubility of EDOT around 20 mM in water.[27] In contrast, EDOT exhibits much higher solubility in organic solvents, which are also often used as electrolytes for electrochemical deposition. Therein, acetonitrile is one of the most commonly used organic solvents for neural electrode coatings deposition.[6,28] Bodart *et al.*[13] found that PEDOT films electrodeposited in acetonitrile had excellent electrochemical properties and a unique porous structure, indicating a significant effect of solvent on the coating properties. In addition to the difference in solubility, acetonitrile has a high polarity that significantly reduces Coulomb repulsion during the cation coupling step, thus avoiding nucleophilic attack on the cationic intermediate and reducing defects during electropolymerization.[29] Moreover, acetonitrile has a wider range of

School of Mechanical Engineering and Automation, Fuzhou University, Fuzhou 350108, China. E-mail: lzli@fzu.edu.cn; mebwhe@fzu.edu.cn

† Electronic supplementary information (ESI) available. See DOI: https://doi.org/10.1039/d4ra03543g

potential window than water.[30,31] Despite the prevalent use of water and acetonitrile in the electrochemical deposition of PEDOT, a comprehensive comparison is lacking regarding the effects of different solvents and EDOT monomer concentrations on the coatings structures and electrochemical performance.

In this study, PEDOT films were electrodeposited in both aqueous and acetonitrile solutions across an extended range of monomer concentrations. The influences of solvents and monomer concentrations on the deposition process were examined by evaluating the current–time transients. Then, the changes in surface morphology, electrochemical performance, and chemical structures of PEDOT coatings were investigated.

2. Experimental

2.1. Electrode preparation

Platinum sheets (purchased from Tengfeng Metal, China) with dimensions of 4 mm × 1.5 mm × 0.2 mm were used as substrates for the electrodeposition of conductive polymer. The platinum sheets on one side were affixed to brass rods with a diameter of 0.8 mm using a conductive silver paste (3813, Ausbond, China). The other side of the Pt sheet was exposed as the electrode surface with an area of 6 mm^2. Silicone rubber (K-705, Kafuter, China) was used for encapsulation in other positions.

2.2. Electrodeposition of PEDOT

The electrodeposition of PEDOT:BF_4(tetrafluoroborate) was conducted with a three-electrode setup using an electrochemical workstation (CHI 660E, Chenhua, China). The Pt sheet served as the working electrode, a titanium sheet (30 mm × 20 mm × 0.3 mm) acted as the counter electrode, and an Ag/AgCl/KCl (aq, saturated) electrode (Type 218, Leici, China) was used as the reference electrode. The electrolyte solutions were prepared by combining 15 mL of the solvent (either water or acetonitrile, Fig. 1a), 120 mM of tetraethylammonium tetrafluoroborate (Aladdin, China), and varying concentrations of EDOT (Acmec, China). Due to the limited solubility of EDOT in deionized water (DIW), monomer concentrations of 1, 5, 10, 15, and 20 mM were used. Conversely, a broader range of EDOT concentrations was employed in acetonitrile (ACN, Aladdin, China) solutions including 1, 10, 20, 50, and 100 mM.

The constant potential method was employed for the electrodeposition of PEDOT. To establish the suitable potential for deposition, cyclic voltammetry was performed within a voltage range from 0 V to 1.5 V at a scan rate of 50 mV s^{-1} (Fig. 1b). The onset oxidation potential was determined from the intersection of the tangents to the baseline current and the slope of the oxidation current.[32,33] Then, the deposition potential was set by adding 0.2 V to this potential.[34] Therefore, the deposition potentials for water solutions with monomer concentrations of 1–20 mM were 1.36, 1.20, 1.15, 1.15, and 1.14 V, respectively, while for acetonitrile solutions with monomer concentrations of 1–100 mM, the deposition potentials were 1.52, 1.52, 1.49, 1.45, and 1.44 V, respectively. The deposition time for all electrodes was 30 seconds. The chronoamperograms during deposition were recorded, and the deposition charge density was obtained by integrating the current density over time.

2.3. Electrochemical characterization

Cyclic voltammetry (CV) and electrochemical impedance spectroscopy (EIS) were conducted utilizing the same three electrodes setup as the electrodeposition process. The same conditions were used to characterize PEDOT films prepared from water and acetonitrile solutions. 0.01 M phosphate buffer solution (PBS) was used as the electrolyte, which was prepared by mixing 100 mL of water with one PBS tablet (P1000, Solarbio, China). The CV was performed in the potential range from −0.6 to 0.8 V at a scan rate of 50 mV s^{-1}. Then, the cathodic charge storage capacity (CSC) was obtained by integrating the cathodic current density over time. For EIS, a 0.01 V root-mean-square sinusoidal signal was used in the range from 0.1 Hz to 100 kHz. The EIS results were fitted to the equivalent circuit[35–37] with Zview (Fig. S-1†).

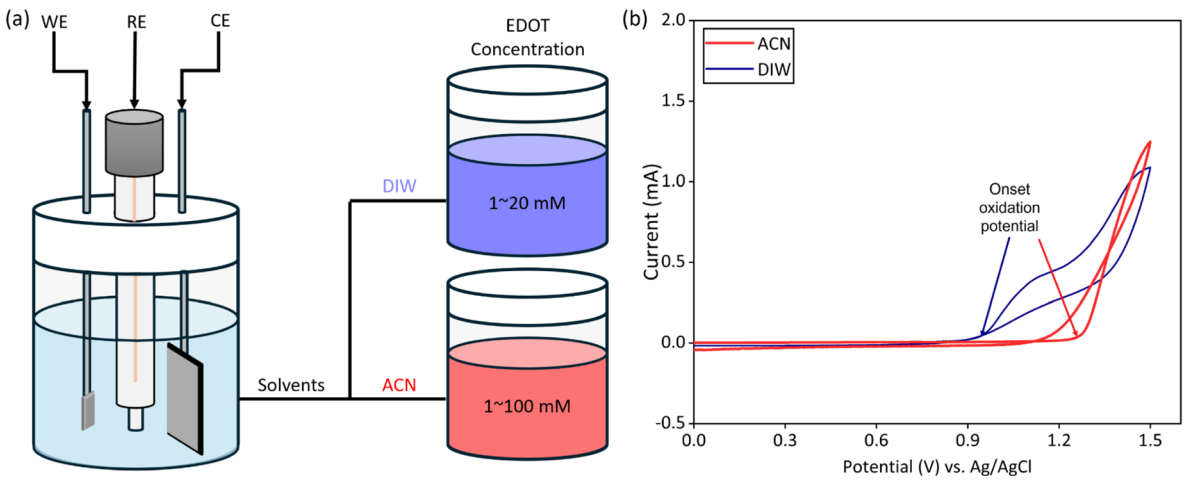

Fig. 1 Electrodeposition diagram. (a) Experimental design. WE, RE, and CE represent working electrode, reference electrode, and counter electrode, respectively. DIW and ACN represent deionized water and acetonitrile. (b) An example to obtain the onset oxidation potential for 20 mM EDOT in the DIW and ACN according to the cyclic voltammograms.

2.4. Surface morphology characterization

The surface morphology of PEDOT was observed by an optical microscope (MV3100, Jiangnan, China) and a scanning electron microscope (SEM 3100, CIQTEK, China) operating at 2.5 kV. The roughness of the PEDOT films was obtained by atomic force microscopy (AFM, Agilent 5500, USA).

2.5. Chemical structures characterization

The chemical structures of the PEDOT films were characterized using Fourier transform infrared (FTIR) spectroscopy (AVATAR360 Intelligent, Nicorette, USA), Raman spectroscopy (Invia Reflex, Renishaw, UK) and UV-visible spectroscopy (Cary 7000, Agilent, USA).

3. Results

3.1. Electrodeposition process of PEDOT films

Fig. 2 showed the first set of cyclic voltammograms to explore the oxidation of EDOT in water and acetonitrile. With the increase of potential, the EDOT was oxidized and the current curve increased significantly, which meant the nucleation of PEDOT. The peak values of current curves increased with rising monomer concentrations in both aqueous and acetonitrile solutions. However, the onset oxidation potential decreased with higher monomer concentrations. In addition, the cross-over could be found in each CV circle for both solutions, resulting in the characteristic "nucleation loop" feature.

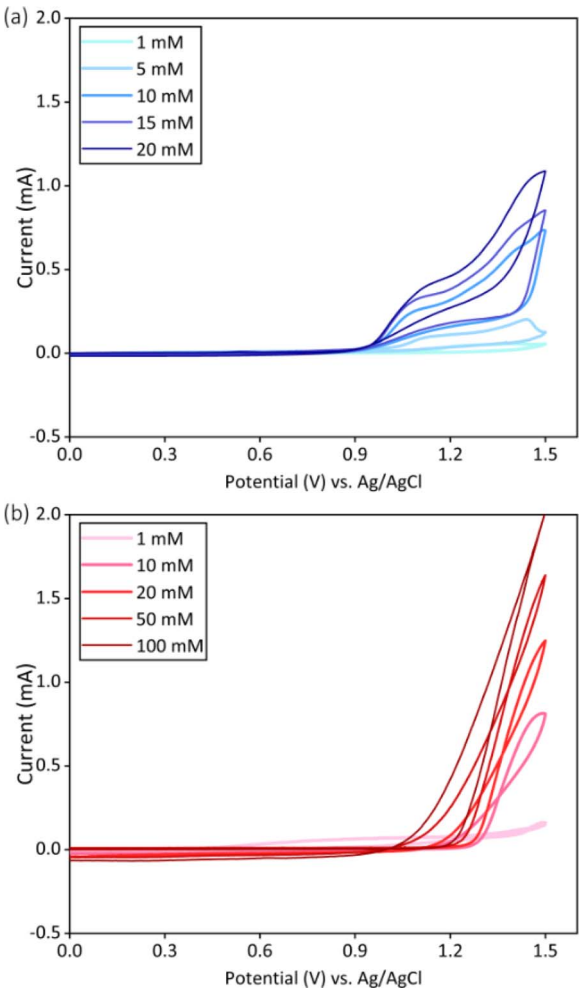

Fig. 2 First set of cyclic voltammetry experiments in (a) water and (b) acetonitrile with different monomer concentrations.

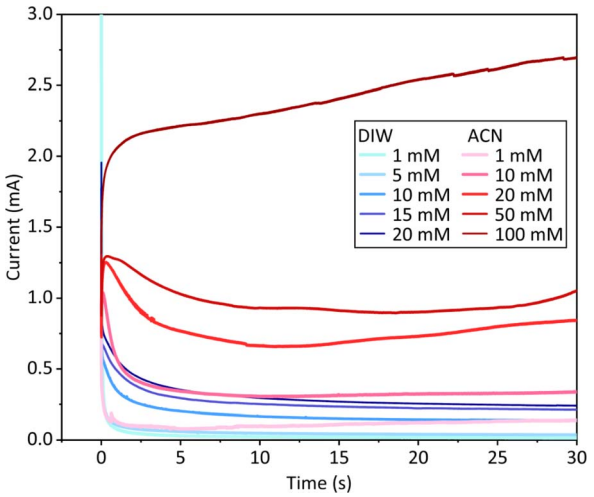

Fig. 3 Chronoamperograms of PEDOT deposition in water and acetonitrile at various monomer concentrations.

Fig. 3 showed the chronoamperograms during PEDOT deposition with varying monomer concentrations. As the monomer concentration increased, the curve amplitude also increased in both aqueous and acetonitrile solutions. Additionally, the current curve in acetonitrile was higher than that in water at the same monomer concentration, which indicated higher deposition charge densities in the acetonitrile solution. During the deposition process, the current curve decreased over time in water. In contrast, the trends of curves in acetonitrile were more complex. For the monomer concentrations ranging from 1 to 50 mM, besides initial transient rise, the current amplitude decreased before increasing; whereas for the monomer concentration at 100 mM, the current consistently rose over time.

3.2. Surface morphology of PEDOT films

Fig. 4 showed the color changes of PEDOT films with various EDOT concentrations. The color of films gradually deepened with the increase of monomer concentrations, which meant the increasing coating thickness.

The surface morphology of PEDOT films under the scanning electron microscope was shown in Fig. 5. For PEDOT films electrodeposited in aqueous solutions, PEDOT did not fully cover the electrode surface at the monomer concentration below 5 mM. At higher concentrations, the PEDOT films became more uniform and exhibited relatively smooth surfaces except some wrinkles. Similarly, as the concentration increased in acetonitrile, PEDOT gradually covered the entire surface except at the low concentration of 1 mM. Notably, the films electrodeposited in acetonitrile possessed a particle texture,

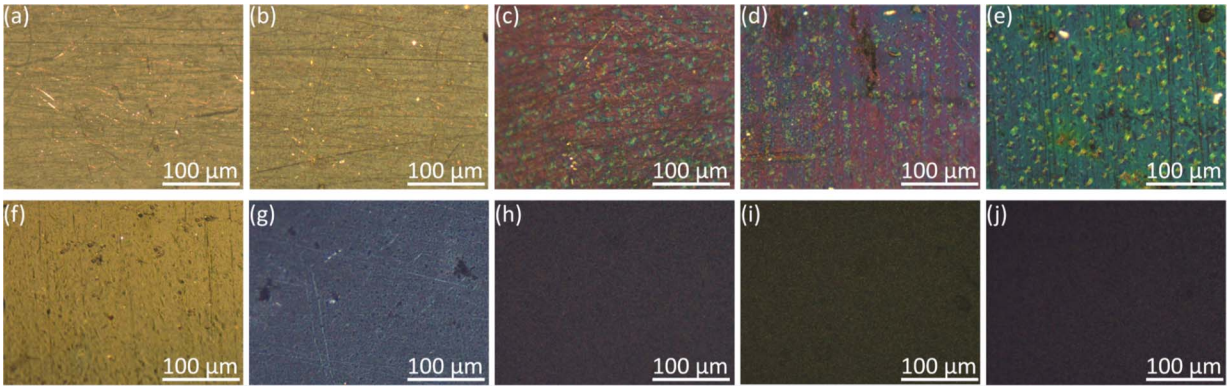

Fig. 4 Optical morphology of PEDOT films deposited in water with EDOT concentration of (a) 1 mM, (b) 5 mM, (c) 10 mM, (d) 15 mM, (e) 20 mM, and PEDOT film deposited in acetonitrile with EDOT concentration of (f) 1 mM, (g) 10 mM, (h) 20 mM, (i) 50 mM, (j) 100 mM.

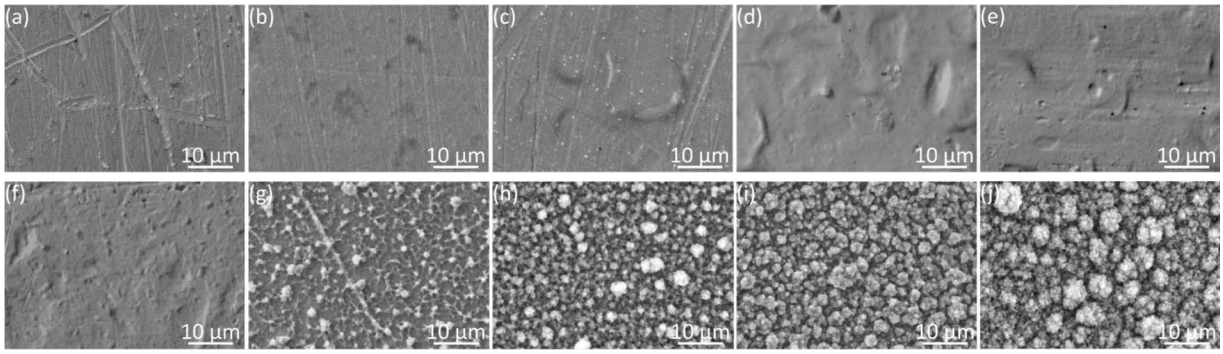

Fig. 5 Scanning electron microscopy of PEDOT films deposited in water with EDOT concentration of (a) 1 mM, (b) 5 mM, (c) 10 mM, (d) 15 mM, (e) 20 mM, and PEDOT film deposited in acetonitrile with EDOT concentration of (f) 1 mM, (g) 10 mM, (h) 20 mM, (i) 50 mM, (j) 100 mM.

resembling the structure of cauliflower. The increasing monomer concentrations from 10 to 100 mM led to denser structures and larger particle sizes.

Fig. 6 showed the roughness of PEDOT films obtained from AFM. It could be found that the roughness of the films deposited in acetonitrile was significantly higher than that of water at the same EDOT concentration. Further, as the monomer concentration increased in either water or acetonitrile, the roughness tended to first increased and then decreased.

3.3. Electrochemical properties of PEDOT films

The cyclic voltammetry curves and charge storage capacity of PEDOT films were shown in Fig. 7. In both solvents, the area enclosed by the CV curve gradually enlarged as the monomer concentration increased (Fig. 7a and b), leading to a risen CSC of the electrode as shown in Fig. 7c. The CSC of electrodes deposited in water exhibited a slower increase with EDOT concentrations, and the CSC value of PEDOT deposited at 20 mM was twice that of before the coating was added. In

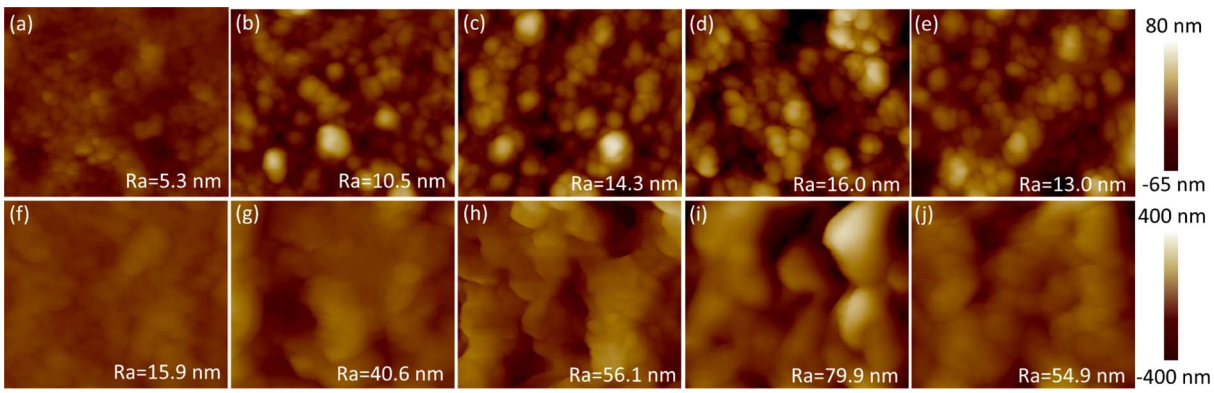

Fig. 6 Atomic force microscopy of PEDOT films deposited in water with EDOT concentration of (a) 1 mM, (b) 5 mM, (c) 10 mM, (d) 15 mM, (e) 20 mM, and PEDOT film deposited in acetonitrile with EDOT concentration of (f) 1 mM, (g) 10 mM, (h) 20 mM, (i) 50 mM, (j) 100 mM.

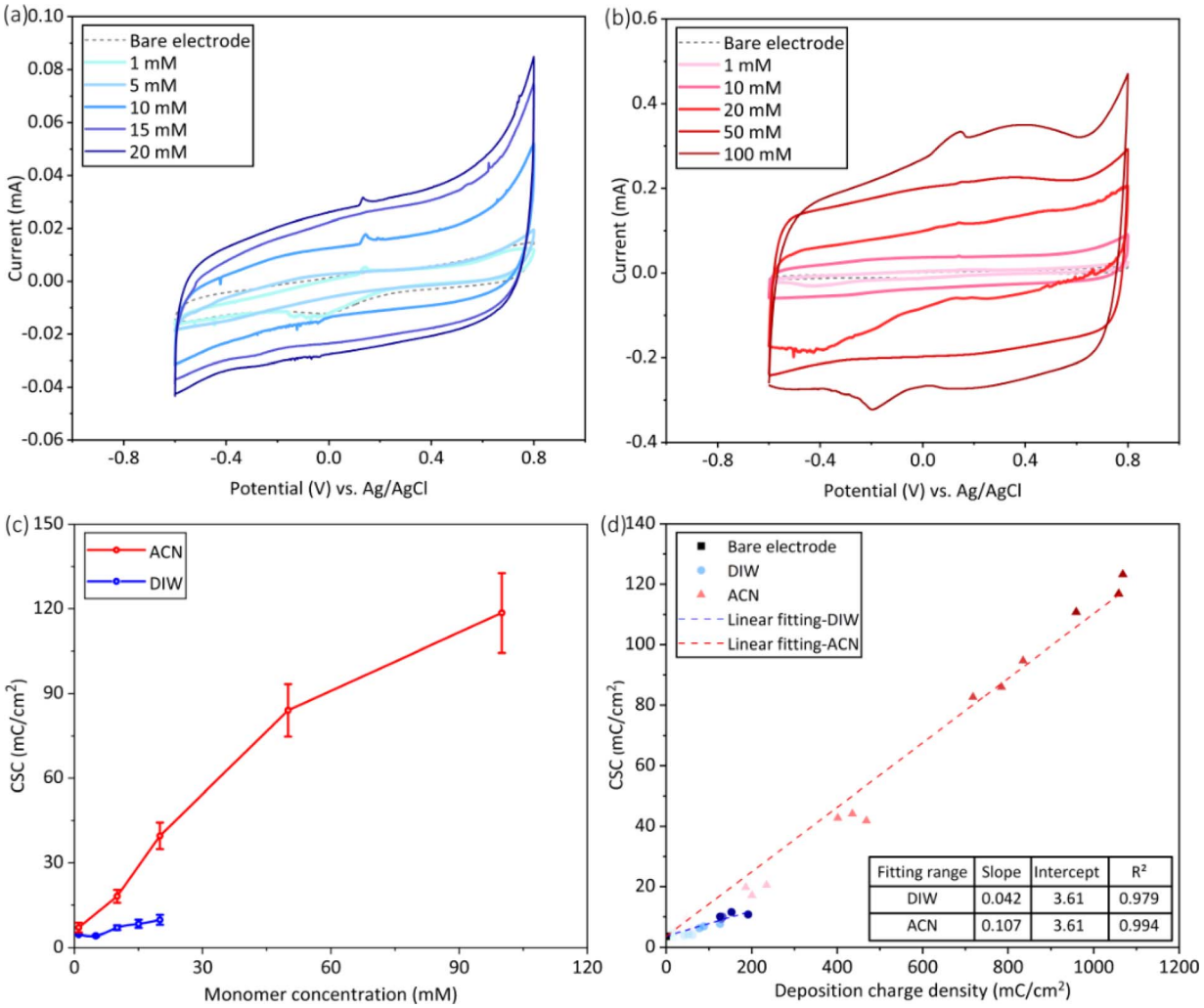

Fig. 7 Electrochemical properties of PEDOT films. (a) CV curves after deposited in water and (b) acetonitrile with different monomer concentrations; (c) plots of CSC *versus* monomer concentration after electrodeposition; (d) plots of CSC of electrodes *versus* deposition charge density.

contrast, when acetonitrile was used, the CSC of the electrode showed a faster increase with rising monomer concentration. The post-deposition CSC of the electrodes were raised to 12 and 35 times at 20 mM and 100 mM of EDOT, respectively. Furthermore, the relationship between the deposited charge density and CSC generally adhered to a linear trend for both PEDOT prepared in DIW and ACN, as shown in Fig. 7d. Notably, the slope of the fitting curves obtained in water and acetonitrile were 0.042 and 0.107, respectively. It meant that the increase rate of the CSC of PEDOT produced in ACN with respect to the deposited charge density was 2.5 times that of the PEDOT produced in DIW.

The EIS curves after electrodeposition were shown in Fig. 8. In both aqueous and acetonitrile solutions, the magnitude of impedance decreased with increasing monomer concentration, and the phase curves shifted to the low frequencies' region (Fig. 8a and b). At the same monomer concentration such as 1 mM, 10 mM, and 20 mM, the PEDOT deposited in acetonitrile had lower impedance magnitude than that of the coatings deposited in water.

The Nyquist plots of PEDOT deposited in water and acetonitrile were shown in Fig. 8c and d, and the results were fitted according to the equivalent circuit in Fig. S-1.† For the PEDOT electrodes prepared at 1 mM of EDOT concentration, Model A was adopted, which was commonly used for Pt electrode. Because the PEDOT film was still very thin and had not cover the whole electrode surface at this condition. As for the PEDOT deposited from other higher EDOT concentrations, Model B was utilized, which was usually used for PEDOT coated Pt electrodes. The fitting results were shown in Table S-1.† The solution resistance R_s, charge transfer resistance R_{ct}, and Warburg impedance Z_w decreased with increasing monomer concentration in both water and acetonitrile, while the capacitance C_d increased at the same time, except that obtained from 1 mM EDOT. Furthermore, lower values of R_s, R_{ct}, and Z_w and higher value of C_d could be found for PEDOT prepared in acetonitrile than those obtained in water at the same EDOT concentration.

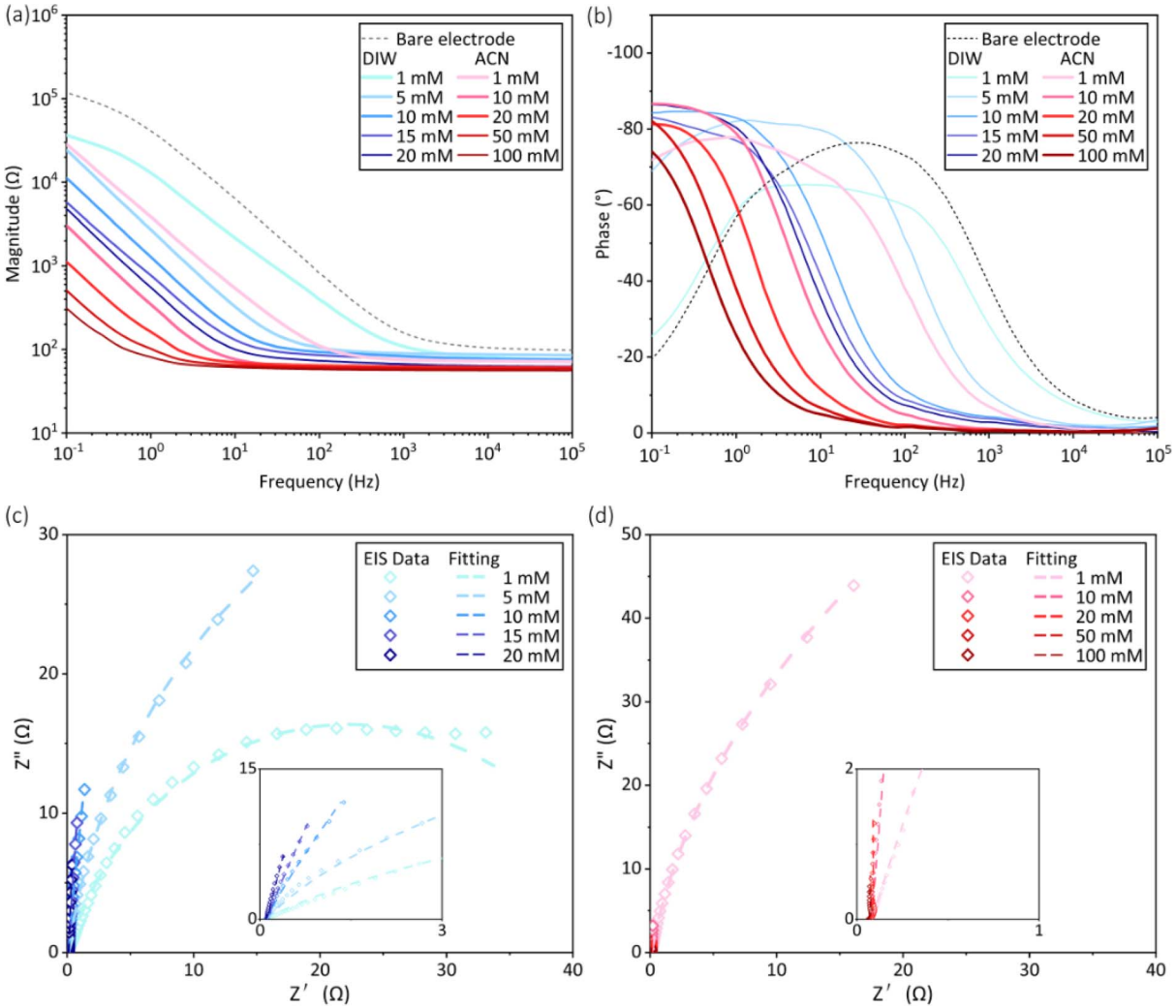

Fig. 8 EIS curves before and after PEDOT deposition. (a) Magnitude curves and (b) phase curves of Bode plot. Nyquist plot in (c) water and (d) acetonitrile including experiment data (shown by points) and fitting results (shown by dash lines).

3.4. Chemical structures of PEDOT films

The FTIR spectroscopy of the PEDOT films were shown in Fig. 9a. The PEDOT prepared in different solvents and EDOT concentrations had similar band positions in spite of some variations in the reflectance. The band at 1445 cm^{-1} was indicative of the C=C bond's stretching. The bands at 1258 cm^{-1} and 1410 cm^{-1} corresponded to C–C in the thiophene ring. The bands at 1011 cm^{-1} and 1078 cm^{-1} were attributed to the presence of C–O bonds in the thiophene ring. The bands at 662 cm^{-1}, 686 cm^{-1}, 699 cm^{-1}, 791 cm^{-1} as well as 864 cm^{-1} were attributed to the C–S–C bonds. And in the EDOT monomer spectra (Fig. S-2a†), a prominent band at 890 cm^{-1} was evident, which corresponds to the C–H bond. However, this band was absent in the PEDOT spectra. These results indicated the successful polymer formation of PEDOT prepared in both aqueous and acetonitrile solutions.

In the Raman spectroscopy results (Fig. 9b), the films electrochemically deposited in water or acetonitrile also showed similar band positions. The bands detected at 1529 cm^{-1} and 1491 cm^{-1} were ascribed to the asymmetric stretching of the C_α=C_β bond, while the symmetric stretching of C_α=C_β bond was indicated by the band at 1417 cm^{-1}. The stretches associated with C_β=$C_{\beta'}$ and C_α=$C_{\alpha'}$ were responsible for the bands at 1365 cm^{-1} and 1256 cm^{-1}. The band at 698 cm^{-1} was characteristic of the C_α–S–$C_{\alpha'}$ vibrations. In addition, the intensity of some bands in the Raman spectroscopy electrodeposited in aqueous solution was higher than that of the films prepared in acetonitrile. In the Raman spectra of the EDOT monomer (Fig. S-2b†), characteristic bands were visible at 1185 cm^{-1} and 1422 cm^{-1}. The comparison of the spectra before and after polymerization showed significant differences.

In the UV-visible spectroscopy (Fig. S-3†), a similar band near 900 nm can be observed for PEDOT synthesized in water and acetonitrile at varying EDOT concentrations, implying the existence of positive polarons. For the bipolarons, it exhibited a band around 1200 nm. Moreover, a distinct broad band at 600 nm was evident, potentially attributed to the π–π* transition of neutral PEDOT.

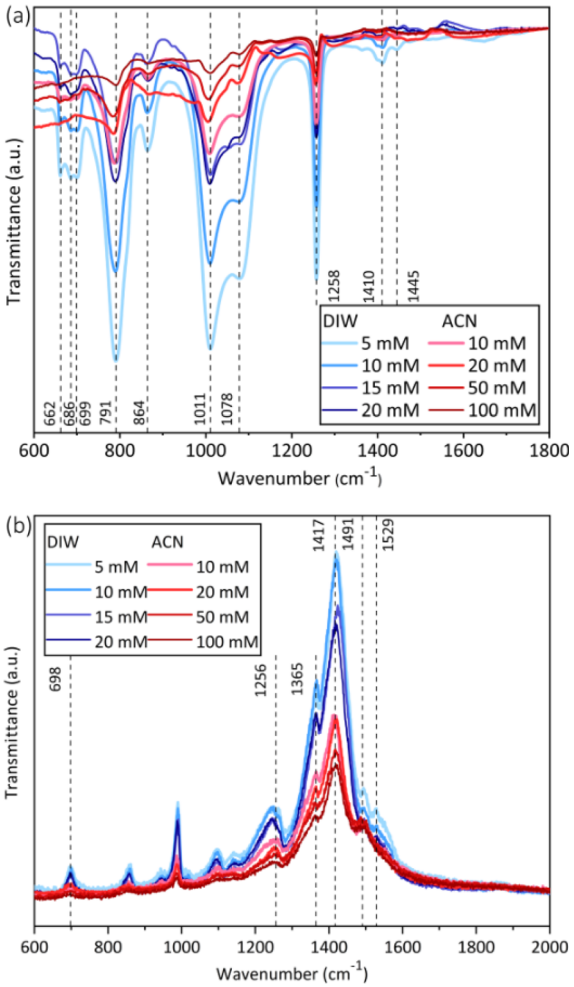

Fig. 9 Comparison of FTIR and Raman spectroscopy after PEDOT electrodeposition in water and acetonitrile at different monomer concentrations. (a) FTIR spectroscopy; (b) Raman spectroscopy.

4. Discussion

Conductive polymers coatings not only have superior electrochemical properties, but also create conditions for the fabrication of multi-modal neural electrodes. Electrodeposition techniques provides an on-site and convenient method for PEDOT preparation.[1] To further understanding the process of PEDOT electrodeposition, in this study the effects of solvents and monomer concentrations on the surface morphology, electrochemical performance, and chemical structures of PEDOT were explored.

The deposition potential plays an important role in the deposition process and properties of PEDOT films. Too low a potential is insufficient for polymerization to form a PEDOT coating, and too high a potential leads to overoxidation, both of which result in impaired electrochemical performance.[38] However, the optimum deposition potential of PEDOT under different conditions varies greatly, and it is affected by various factors such as solvent type, monomer concentration and surface morphology. Employing cyclic voltammetry to obtain the onset oxidation potential of PEDOT under various conditions, followed by applying a uniform voltage bias, offers a convenient and effective alternative method[34,39] (Fig. 2). By adopting this approach, this study has explored the effects of monomer concentration and solvent, contributing to an understanding of the factors affecting PEDOT deposition and facilitating parameter optimization. Nonetheless, further investigation deserves to be conduct to obtain the optimal combination of deposition conditions.

Before deposition, onset oxidation potential of EDOT could be obtained through CV scanning (Fig. 2).[24,32,33] It was found that the onset oxidation potential changed with the solvents and EDOT concentrations. Therein, a higher onset oxidation potential was required when using acetonitrile compared to water. It may result from the need for a strong enough base to remove protons generated during PEDOT polymerization,[29] a condition met by water but not by acetonitrile.[13] Consequently, a higher potential is necessary to oxidize the protons and facilitate the subsequent steps of polymerization in acetonitrile solutions. Additionally, nucleation loops can be observed in both solvents (Fig. 2), which is usually observed during the first cyclic voltammetry of the electrodeposition and indicates the onset of nucleation.[29,40] This phenomenon is due to the slow formation of redox intermediates in the diffusion layer in front of the working electrode, which are subsequently oxidized to charged mono- or dications.[29,40]

The analysis of current–time transients during electrodeposition provided insight into the factors governing the growth mechanism under various conditions. Electrodeposition conducted in an aqueous environment resulted in similar developing trends in the chronoamperograms curves (Fig. 3). They all exhibited a declining trend, which suggested that diffusion controlled processes predominantly influenced the deposition dynamics.[26] Conversely, the curves obtained in acetonitrile were more complex. At monomer concentrations ranging from 1 to 50 mM, the curves initially ascended due to the double layer charging. Then, there was a descend before rising again, a pattern indicative of the interplay between diffusion and charge control mechanisms.[24] However, when the monomer concentration reached 100 mM, the chronoamperogram curve consistently sloped upwards. This could be attributed to the diminished influence of diffusion control, leading to a dominance of charge control in the deposition process.

Enhancing the electrochemical performance of electrodes is critical for PEDOT modified electrodes. The study found that, in both aqueous and acetonitrile solutions, an increase in monomer concentration led to a rise in charge storage capacity and a decrease in impedance magnitude post-electrodeposition (Fig. 7 and 8). This is consistent with the results of Kulandaivalu *et al.*[18] for EDOT concentrations ranging from 1 to 10 mM in aqueous solutions. On the other hand, PEDOT prepared in acetonitrile exhibited a more rapid increase in the CSC as a function of the monomer concentration. More essentially, the deposited charge density affected the thickness and electrochemical properties of PEDOT. Recently, Niederhoffer *et al.*[28] reviewed the literature on the electrochemical deposition of PEDOT and proposed that coating thickness and charge storage

capacity were positively related to the deposition charge density. However, to the best of our knowledge, direct comparisons of solvent effects have been lacking before. In this study, it was found that the solvent played an important role in the relationship between the deposition charge density and the resulting CSC (Fig. 7d). Moreover, according to the fitting results, the utilization of acetonitrile and the elevation in monomer concentration significantly mitigated the charge transfer resistance R_{ct} as well as the finite-length Warburg diffusion impedance Z_w, while simultaneously enhanced the double layer capacitance C_d, consequently leading to a decrease in the electrode impedance.

The changes in electrochemical properties after deposition could also be reflected by the various surface morphology. Inspection under a scanning electron microscope revealed that PEDOT films formed in an aqueous environment showed a dense and smooth surface, while PEDOT prepared in acetonitrile exhibited a porous morphology (Fig. 5). Belaidi *et al.*[11] reported a similar phenomenon and attributed these results to the higher dielectric constant of water and the possible higher solubility of the oligomers in water due to the presence of the dopant anion. This increased solubility was anticipated to slow down the deposition rate and facilitated the creation of more extensive polymer chains, culminating in a smoother film texture. Additionally, water's role in aiding proton removal during PEDOT growth likely contributed to the development of more extensive polymer chains within the electrodeposited PEDOT, resulting in a smoother surface.[13,29] In contrast, a porous morphology of PEDOT was formed in acetonitrile. As the EDOT concentration was elevated in either water or acetonitrile, the surface roughness exhibited a comparable pattern of first increase followed by subsequent decrease. This phenomenon was similar to the variation of roughness under different deposition times,[41] which could be attributed to PEDOT gradually covering the entire surface.

The band positions in FTIR and Raman spectroscopy from the two solvents exhibited no significant discrepancies, which was consistent with the results of PEDOT deposited in water and methylene chloride.[42] After polymerization, the distinctive band at 890 cm^{-1} associated with the C–H bond in the EDOT monomer was absent in the FTIR spectroscopy (Fig. 9a and S-2a†), as reported by prior studies.[43,44] As for the EDOT monomer in Raman spectroscopy, characteristic bands such as 1185 cm^{-1} and 1422 cm^{-1} can be observed, similar to those documented in the literature[45] (Fig. S-2b†). Notably, the band around 1417 cm^{-1} became especially obvious in the Raman spectrum of PEDOT (Fig. 9b), corresponding to the $C_\alpha{=}C_\beta$ bond within the thiophene ring.[45] These results indicate the successful polymerization of PEDOT films on the platinum substrate. Additionally, the variation in the intensity of characteristic bands could be found for PEDOT films prepared in the two solvents, potentially attributable to the protic nature of the aqueous solution.[33,46]

In this study, to facilitate the direct comparison of electrochemically deposited PEDOT in water and acetonitrile, an Ag/AgCl/KCl (aq, saturated) electrode was used as a reference electrode in both solvents. However, the use of an aqueous reference electrode such as Ag/AgCl/KCl (aq, saturated) in acetonitrile may lead to solution contamination and potential fluctuations. To verify the potential fluctuation, open circuit potentials (OCP) were monitored in acetonitrile and water. It was found that the OCP fluctuation was within 5 mV in 5 minutes (Fig. S-4†), which may be related to the short time of use in acetonitrile. Nevertheless, using an Ag quasi-reference electrode in acetonitrile can help reduce potential fluctuations of the Ag/AgCl electrode in long-term applications.

The stability of PEDOT coatings has also been a great concern in recent years. Noble metals like Pt, or Au are frequently used as neural electrode substrates. However, they are incapable of forming stable covalent bonds with polymer coatings.[47] To solve this problem, physical techniques have been proposed to create micro–nanostructures to enhance mechanical anchoring, while chemical methods have been used to introduce intermediate adhesion layers to enhance the adhesion of the coating.[48,49] Recent works also suggests that deposition in acetonitrile is more conducive to improving the stability of the coating.[13,19] However, there are many factors that affect the stability of the PEDOT coating, such as electrode geometry, surface morphology, *etc.* The effect of different solvents on the stability of the coating deserves further exploration in the future work.

5. Conclusions

PEDOT films deposited in water and acetonitrile showed an increase in CSC with increasing monomer concentration, accompanied by a decrease in impedance magnitude. A generally linear relationship was observed between the CSC of PEDOT prepared in either solvent and the deposition charge density. Notably, the CSC increase rate relative to deposition charge density of PEDOT synthesized in acetonitrile was 2.5 times that achieved in aqueous solutions. These results could help to guide the deposition of PEDOT coatings on neural electrode interfaces.

Data availability

The authors confirm that the data supporting the findings of this study are available within the article.

Conflicts of interest

The authors declare no competing interests.

Acknowledgements

This research was funded by Natural Science Foundation of Fujian Province of China under Grant Number 2023J05097 and the Young and Middle-aged Teacher Education Research Project of the Education Department of Fujian Province of China under Grant Number JAT220004. The authors acknowledge the support from Fujian College Association Instrumental Analysis Center of Fuzhou University.

References

1 C. Boehler, S. Carli, L. Fadiga, T. Stieglitz and M. Asplund, Tutorial: guidelines for standardized performance tests for electrodes intended for neural interfaces and bioelectronics, *Nat. Protoc.*, 2020, **15**, 3557–3578.
2 H. S. Mandal, J. S. Kastee, D. G. McHail, J. F. Rubinson, J. J. Pancrazio and T. C. Dumas, Improved poly(3,4-ethylenedioxythiophene) (PEDOT) for neural stimulation, *Neuromodulation*, 2015, **18**, 657–663.
3 D. T. Simon, E. O. Gabrielsson, K. Tybrandt and M. Berggren, Organic bioelectronics: bridging the signaling gap between biology and technology, *Chem. Rev.*, 2016, **116**, 13009–13041.
4 Y. Shi, R. Liu, L. He, H. Feng, Y. Li and Z. Li, Recent development of implantable and flexible nerve electrodes, *Smart Mater. Med.*, 2020, **1**, 131–147.
5 L. Ricotti and A. Menciassi, Engineering stem cells for future medicine, *IEEE Trans. Biomed. Eng.*, 2013, **60**, 727–734.
6 N. Rossetti, J. Hagler, P. Kateb and F. Cicoira, Neural and electromyography PEDOT electrodes for invasive stimulation and recording, *J. Mater. Chem. C*, 2021, **9**, 7243–7263.
7 J. Leal, S. Shaner, L. Matter, C. Böhler and M. Asplund, Guide to leveraging conducting polymers and hydrogels for direct current stimulation, *Adv. Mater.*, 2023, **10**, 2202041.
8 R. Green and M. R. Abidian, Conducting polymers for neural prosthetic and neural interface applications, *Adv. Mater.*, 2015, **27**, 7620–7637.
9 J. A. Goding, A. D. Gilmour, U. A. Aregueta Robles, E. A. Hasan and R. A. Green, Living bioelectronics: strategies for developing an effective long-term implant with functional neural connections, *Adv. Funct. Mater.*, 2018, **28**, 1702969.
10 G. Xu, B. Li, X. T. Cui, L. Ling and X. Luo, Electrodeposited conducting polymer PEDOT doped with pure carbon nanotubes for the detection of dopamine in the presence of ascorbic acid, *Sens. Actuators, B*, 2013, **188**, 405–410.
11 F. S. Belaidi, A. Civélas, V. Castagnola, A. Tsopela, L. Mazenq, P. Gros, J. Launay and P. Temple-Boyer, PEDOT-modified integrated microelectrodes for the detection of ascorbic acid, dopamine and uric acid, *Sens. Actuators, B*, 2015, **214**, 1–9.
12 V. Durairaj, N. Wester, J. Etula, T. Laurila, J. Lehtonen, O. J. Rojas, N. Pahimanolis and J. Koskinen, Multiwalled carbon nanotubes/nanofibrillar cellulose/Nafion composite-modified tetrahedral amorphous carbon electrodes for selective dopamine detection, *J. Phys. Chem. C*, 2019, **123**, 24826–24836.
13 C. Bodart, N. Rossetti, J. E. Hagler, P. Chevreau, D. Chhin, F. Soavi, S. B. Schougaard, F. Amzica and F. Cicoira, Electropolymerized poly(3,4-ethylenedioxythiophene) (PEDOT) coatings for implantable deep-brain-stimulating microelectrodes, *ACS Appl. Mater. Interfaces*, 2019, **11**, 17226–17233.
14 L. V. Kayser and D. J. Lipomi, Stretchable conductive polymers and composites based on PEDOT and PEDOT:PSS, *Adv. Mater.*, 2019, **31**, 1806133.
15 M. J. Donahue, A. Sanchez-Sanchez, S. Inal, J. Qu, R. M. Owens, D. Mecerreyes, G. G. Malliaras and D. C. Martin, Tailoring PEDOT properties for applications in bioelectronics, *Mater. Sci. Eng., R*, 2020, **140**, 100546.
16 F. Wang, X. Zhang, Y. Ma and W. Yang, Synthesis of HNTs@PEDOT composites via in situ chemical oxidative polymerization and their application in electrode materials, *Appl. Surf. Sci.*, 2018, **427**, 1038–1045.
17 G. Drewelow, H. Wook Song, Z. Jiang and S. Lee, Factors controlling conductivity of PEDOT deposited using oxidative chemical vapor deposition, *Appl. Surf. Sci.*, 2020, **501**, 144105.
18 S. Kulandaivalu, Z. Zainal and Y. Sulaiman, Influence of monomer concentration on the morphologies and electrochemical properties of PEDOT, PANI, and PPy prepared from aqueous solution, *Int. J. Polym. Sci.*, 2016, **2016**, 1–12.
19 N. Rossetti, P. Luthra, J. E. Hagler, A. H. Jae Lee, C. Bodart, X. Li, G. Ducharme, F. Soavi, B. Amilhon and F. Cicoira, Poly(3,4-ethylenedioxythiophene) (PEDOT) coatings for high-quality electromyography recording, *ACS Appl. Bio Mater.*, 2019, **2**, 5154–5163.
20 H. Jiang, W. Wu, Z. Chang, H. Zeng, R. Liang, W. Zhang, W. Zhang, G. Wu, Z. Li and H. Wang, In situ polymerization of PEDOT: PSS films based on EMI-TFSI and the analysis of electrochromic performance, *e-Polym.*, 2021, **1**, 722–733.
21 S. Lupu, In situ electrochemical preparation and characterization of PEDOT–Prussian blue composite materials, *Synth. Met.*, 2011, **161**, 384–390.
22 H. Chul Lim, S. J. Jang, Y. Cho, H. Cho, G. Venkataprasad, V. Vinothkumar, I. S. Shin and T. Hyun Kim, Graphene quantum dot-doped PEDOT for simultaneous determination of ascorbic acid, dopamine, and uric acid, *ChemElectroChem*, 2022, **9**, e202200835.
23 S. A. Spanninga, D. C. Martin and Z. Chen, X-ray photoelectron spectroscopy study of counterion incorporation in poly(3,4-ethylenedioxythiophene) (PEDOT) 2: polyanion effect, toluenesulfonate, and small anions, *J. Phys. Chem. C*, 2010, **114**, 14992–14997.
24 E. Tamburri, S. Orlanducci, F. Toschi, M. L. Terranova and D. Passeri, Growth mechanisms, morphology, and electroactivity of PEDOT layers produced by electrochemical routes in aqueous medium, *Synth. Met.*, 2009, **159**, 406–414.
25 T. Marek, G. Orbán, D. Meszéna, G. Márton, I. Ulbert, G. Mészáros and Z. Keresztes, Optimization aspects of electrodeposition of photoluminescent conductive polymer layer onto neural microelectrode arrays, *Chem. Phys.*, 2021, **260**, 124163.
26 H. Mousavi, L. M. Ferrari, A. Whiteley and E. Ismailova, Kinetics and physicochemical characteristics of electrodeposited PEDOT:PSS thin film growth, *Adv. Mater.*, 2023, **9**, 2201282.

27 L. Duan, Y. Zhao, F. Guo, W. Liu, C. Hou and Z. Ni, Enzymatic-catalyzed polymerization of water-soluble electrically conductive polymer PEDOT:PSS, *Polym. Adv. Technol.*, 2014, **25**, 896–899.

28 T. Niederhoffer, A. Vanhoestenberghe and H. T. Lancashire, Methods of poly(3,4)-ethylenedioxithiophene (PEDOT) electrodeposition on metal electrodes for neural stimulation and recording, *J. Neural Eng.*, 2023, **20**, 011002.

29 J. Heinze, B. A. Frontana-Uribe and S. Ludwigs, Electrochemistry of conducting polymers—persistent models and new concepts, *Chem. Rev.*, 2010, **110**, 4724–4771.

30 T. Mairegger, H. Li, C. Grießer, D. Winkler, J. Filser, N. G. Hörmann, K. Reuter and J. Kunze-Liebhäuser, Electroreduction of CO_2 in a non-aqueous electrolyte-the generic role of acetonitrile, *ACS Catal.*, 2023, **13**, 5780–5786.

31 Q. Mi, R. H. Coridan, B. S. Brunschwig, H. B. Gray and N. S. Lewis, Photoelectrochemical oxidation of anions by WO_3 in aqueous and nonaqueous electrolytes, *Energy Environ. Sci.*, 2013, **6**, 2646.

32 N. A. Zubair, N. A. Rahman, H. N. Lim and Y. Sulaiman, Production of conductive PEDOT-coated PVA-GO composite nanofibers, *Nanoscale Res. Lett.*, 2017, **12**, 113.

33 Y. Seki, M. Takahashi and M. Takashiri, Effects of different electrolytes and film thicknesses on structural and thermoelectric properties of electropolymerized poly(3,4-ethylenedioxythiophene) films, *RSC Adv.*, 2019, **9**, 15957–15965.

34 H. Liu, W. Zhou, X. Ma, S. Chen, S. Ming, K. Lin, B. Lu and J. Xu, Capacitive performance of electrodeposited PEDOS and a comparative study with PEDOT, *Electrochim. Acta*, 2016, **220**, 340–346.

35 M. Ganji, A. T. Elthakeb, A. Tanaka, V. Gilja, E. Halgren and S. A. Dayeh, Scaling Effects on the electrochemical performance of poly(3,4-ethylenedioxythiophene) (PEDOT), Au, and Pt for electrocorticography recording, *Adv. Funct. Mater.*, 2017, **27**, 1703018.

36 P. Wanga and W. L. Olbricht, PEDOT/Nafion composite thin films supported on Pt electrodes: Facile fabrication and electrochemical activities, *Chem. Eng. J.*, 2010, **16**, 383–390.

37 G. Yuea, D. Zhanga, F. Tana, J. Wub, F. Lia, C. Chena and Z. Lan, Enhanced performance of dye-sensitized solar cells based on anelectrodeposited-poly(3,4 ethylenedioxythiophene)/platinumcomposite counter electrode, *Synth. Met.*, 2014, **197**, 204–209.

38 N. Azman, H. Lim and Y. Sulaiman, Effect of electropolymerization potential on the preparation of PEDOT/graphene oxide hybrid material for supercapacitor application, *Electrochim. Acta*, 2016, **188**, 785–792.

39 N. Gao and X. Huang, Electropolymerization of EDOT in an anionic surfactant-stabilized hydrophobic ionic liquid-based microemulsion, *Phys. Chem. Chem. Phys.*, 2022, **24**, 13793–13805.

40 J. Heinze, A. Rasche, M. Pagels and B. Geschke, On the origin of the so-called nucleation loop during electropolymerization of conducting polymers, *J. Phys. Chem. B*, 2007, **111**, 989–997.

41 Y. Zhang, Y. Chen, S. Contera and R. G. Compton, Electrochemical and nanostructural characterization of poly (3, 4-ethylenedioxythiophene): poly (styrenesulfonate) films as coatings for neural electrodes, *ACS Appl. Polym. Mater.*, 2023, **5**, 5555–5566.

42 S. Wustoni, G. Nikiforidis, S. Inal, Y. S. Indartono, V. Suendo and B. Yuliarto, Hydroxymethyl PEDOT microstructure-based electrodes for high-performance supercapacitors, *APL Mater.*, 2022, **10**, 61101.

43 S. Selvaganesh, J. Mathiyarasu, K. Phani and V. Yegnaraman, Chemical synthesis of PEDOT–Au nanocomposite, *Nanoscale Res. Lett.*, 2007, **2**, 546.

44 A. Diah, A. Wirayudha, S. Supriadi and T. Santoso, The length of reaction time on the synthesis of poly (3, 4-ethylenedioxythiophene), *J. Phys.: Conf. Ser.*, 2021, **1763**, 012079.

45 K. Nitta, M. Tsumaki, T. Kawano, K. Terashima and T. Ito, Printing PEDOT from EDOT via plasma-assisted inkjet printing, *J. Phys. D: Appl. Phys.*, 2019, **52**, 315202.

46 C. KvarnstroÈm, H. Neugebauer, S. Blomquist, H. J. Ahonen, J. Kankare and A. Ivaska, In situ spectroelectrochemical characterization of poly(3,4-ethylenedioxythiophene), *Electrochim. Acta*, 1999, **44**, 2739–2750.

47 C. Boehler, F. Oberueber, S. Schlabach, T. Stieglitz and M. Asplund, Long-term stable adhesion for conducting polymers in biomedical applications: IrOx and nanostructured platinum solve the chronic challenge, *ACS Appl. Mater. Interfaces*, 2017, **9**, 189–197.

48 A. Pranti, A. Schander, A. Bödecker and W. Lang, PEDOT: PSS coating on gold microelectrodes with excellent stability and high charge injection capacity for chronic neural interfaces, *Sens. Actuators, B*, 2018, **275**, 382–393.

49 O. Y. Liangqi, W. Bin, K. Chin-chen, P. Sheevangi, F. Brendan and M. David, Enhanced PEDOT adhesion on solid substrates with electrografted P(EDOT-NH_2), *Sci. Adv.*, 2017, **3**, e1600448.